Modeling and Analysis of a Permanent Magnet Synchronous Generator Dedicated to Wind Energy Conversion

*Tola, O. J[1], Umoh, E. A[2]
[1]Electrical and Electronics Engineering Department, Federal University of Technology, PMB 65 Minna Niger State, Nigeria
[2]Department of Electrical Engineering Technology, Federal Polytechnic, Kaura Namoda Zamfara State, Nigeria
*Corresponding author email: omokhafe@gmail.com, +2348063148163

ABSTRACT
In this paper, the modeling and finite element analysis of a three-phase radial flux permanent magnet synchronous generator (PMSG) for dedicated wind energy conversion is presented. The generator is for use with direct drive wind turbine. A mathematical model in the rotor reference frame of the machine is formulated and a 2D model of PMSG is designed using ANSYS Maxwell software. Two PM materials - Neodymium-Iron-Boron (Nd-Fe-B) and Alnico (Al, Ni, Co, Fe) were considered in the analysis of the PMSG for wind turbine, and a comparative analysis was carried out using the method of finite element field analysis. The numerical results obtained shows that Alnico material has a better torque performance. The accuracy of the model was validated by the formation of the magnetic field lines and flux density distribution of PMSG.

Keywords: *Finite element analysis, PMSG, cogging torque, wind energy conversion.*

1 INTRODUCTION

In many countries of the world, there are remote communities where connection to the national grid is too expensive and diesel generating sets as an alternative source of power generation are too expensive. Under such circumstances, a locally built small-scale stand-alone distributed generation system could be a viable source of electricity generation to the communities. The wind power system is among the pollution-free renewable energy sources and is considered as one of the most viable types of renewable power solutions to the remote consumers.

Induction generator has received considerable interest from many researchers (Pena, Cardenas, Asher, & Clare, 2000), due to their simplicity in construction, robustness, low cost and nearly maintenance-free operation. They are used where high power ratings are required, whereas for small portable power sources for remote areas, radial PMSG are employed. Potentially, the PMSG offer a higher efficiency, improvement in the thermal characteristics due to the absence of field, losses, high reliability due to the absence of mechanical components such as slip rings and higher power – to - weight ratio, compared to an induction generator (Ionel & Popescu, 2009; Jeong, Sul, Schulz, & Patel, 2005). The major drawbacks are the high cost of permanent magnet (PM) materials and demagnetization of PM at high temperatures. However, in recent years, the cost of PM materials has decreased (Li & Chen, 2008). This paper presents the modeling and electromagnetic analysis of a small wind PMSG for stand-alone power generation using the ANSYS Maxwell software. The generator model is compact and light, and can therefore be conveniently installed on the top of the tower and couple directly to the wind turbine (WT) without the need for a gear box.

Various PM machine topologies have been proposed in the literature for direct-coupled wind generators, namely inner and outer rotors (see Figure 1) (J. Y. Chen, Nayar, & Xu, 1998). In the outer rotor, the wound stator is stationary and located in the center of the machine while the magnets are mounted along the inner circumference of the rotating rotor. The main advantages of outer rotor structure are that the rotor is furnished with a higher number of poles and can provide good support for the PMs, while the inner rotor structure offers a better cooling for the stator armature winding (Chalmers, Wu, & Spooner, 1999; J. Y. Chen et al., 1998; Parviainen, Pyrhönen, & Kontkanen, 2005).

Many manufacturers of small wind turbine prefer the direct-coupled PMSGs to the conventional gearbox-coupled wind turbine because a direct-coupled generator eliminates mechanical reduction gear, reduces size of the overall system and lowers installation and maintenance costs and noise. However, the direct-coupled generator requires a large number of magnetic poles and has to operate at very low speeds (from 200 r/min to 600 r/min) in order to match the wind turbine speed and also generate power within a suitable range of frequency (25 – 70 Hz) (Chan & Lai, 2007). The higher the frequency, the smaller the matching transformer. Gearless systems are also preferred due to their cost, size and reliability (Lampola & Perho, 1996). The air gap orientation of PMSG are axial flux (with disc type) and radial flux (with cylindrical rotor). If the flux direction is parallel with the air gap axis, it is axial and if it is perpendicular to the axis of the air gap, the machine is radial (Gieras & Wing, 2002). Axial flux machines are known for having a higher torque density than radial flux machines. But the main advantages of radial flux machines are the low cost of production and the length of the stator and the air gap diameter which can be chosen independently (Cavagnino, Lazzari, Profumo, & Tenconi, 2002; Parviainen et al., 2005).

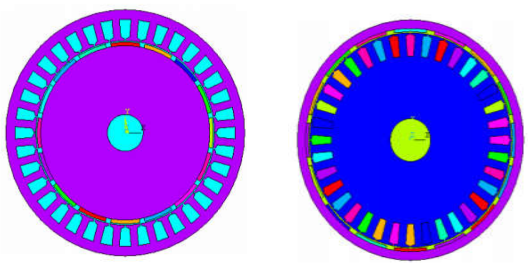

(a) Inner rotor (b) Outer rotor

Figure 1: Radial flux PM wind generator (Y. Chen, Pillay, & Khan, 2004)

The schematic diagram of PMSG based wind turbine is shown in Figure 2, in which a variable speed wind turbine PMSG is connected to a dedicated load via a converter.

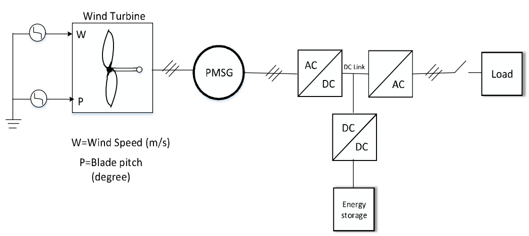

Figure 2: schematic diagram of PMSG based wind turbine

2 MODEL OF THE GENERATOR

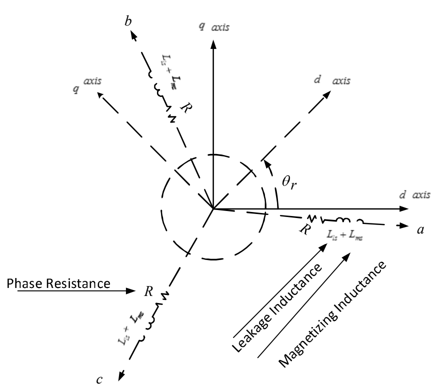

Figure 3: Relationship among stationary abc phase and d-q axes

Figure 3 shows the relationship among the phases abc stationary and rotor $d-q$ axes. R is the phase resistance, while L_m and L_{ls} are the magnetizing and leakage inductance respectively. From Figure 3, the $d-q$ voltage equation in the rotor reference frame can be obtained.

The model voltage equations of PMSG expressed in d-q reference frame is given as follows (Kyoung-Jin KoI, Seok-Myeong JangI, Ji-Hoon ParkI, Han-Wook ChoI, & Dae-Joon YouP, 2011).

$$\begin{cases} V_d = -R_s i_d - p\lambda_d + \omega\lambda_q \\ V_q = -R_s i_q - p\lambda_q - \omega\lambda_d \end{cases} \quad (1)$$

Where

$$p\lambda_d = L_d \frac{di_d}{dt} \text{ and } p\lambda_q = L_q \frac{di_q}{dt}$$

The coupling electromagnetic or flux linkage equation

$$\begin{cases} \lambda_d = L_d i_d + \lambda_m \\ \lambda_q = L_q i_q \end{cases} \quad (2)$$

L_d is the stator inductance in d-axis (H)

L_q is the stator inductance in q-axis (H)

λ_m is the magnet flux linkage

The Torque expression is given as

$$T_{em} = \frac{3p}{2}\left(\left(L_d - L_q\right)i_d i_q + i_q \lambda_m\right) \quad (3)$$

Copper losses

The principal losses of the generator are the copper loss, it can be written as

$$P_{cu} = \frac{3}{2} R_s \left(i_d^2 + i_q^2\right) \quad (4)$$

The input power equation, neglecting core losses, can be calculated by

$$\mathrm{P}_{in} = \frac{3}{2}\left(V_d i_d + V_q i_q\right) + \frac{3}{2} R_s \left(i_d^2 + i_q^2\right) \quad (5)$$

The output power of the generator is given as (Ong, 1998).

$$\mathrm{P}_o = \frac{3}{2}\left(V_d i_d + V_q i_q\right) - \frac{3}{2} R_s \left(i_d^2 + i_q^2\right) - \frac{3}{4}\lambda\left(i_d^2 + i_q^2\right) \quad (6)$$

Hence the $d-q$ model of PMSG has been developed in the rotor reference frame.

Finite Element Modeling of PMSG

A numerical technique for solving engineering field problems, which involves differential equations applied over regions, constrained by boundary conditions is known as finite element method (FEM). The purpose of using finite element method is to make the overall structure discrete by using limited units to represent complex objects. The units are connected with a finite number of nodes. By choosing appropriate boundary conditions of the model, a good solution of the model can be obtained. FEM was first proposed in the 1940s by Courant, who utilized the Ritz method of numerical analysis to obtain approximate solutions to vibration systems (Sarhan M. Musa, 2012). FEM have been used extensively to solve engineering problems due to its accessibility and accurate results. And in recent times, it has been widely recognized as a general method for the design and analysis of different type of permanent magnet machines.

In this work, the ANSYS Maxwell software package was used for the finite element analysis (FEA) to solve magnetic and electric field problems. The FEM design of PMSG includes the structure type, material selection and geometry of the model, i.e. outer and inner diameters of the stator and rotor, air gap, length-width-thickness of PMs, size of the slot and data of winding. The procedure involves seven steps:

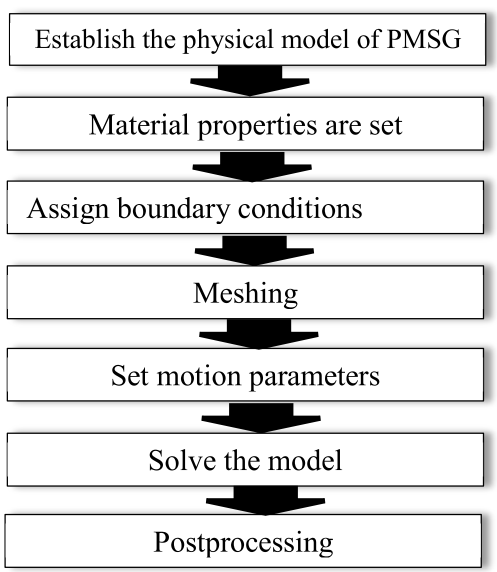

Figure 4. Procedure for FEM of PMSG

Geometric Dimension and Parameters of PMSG

Table I show the parameters of the PMSG model used in the analysis. The 2D finite element is set up according to the parameters in Table I. The 2D model is shown in Figure 1.

Table I: Parameters of PMSG

Parameters	Values	Unit
Rated Output Power	0.1	kW
Rated Voltage	24	V
Rated Speed	1500	rpm
Number of Poles	30	
Outer Diameter of Stator	105	mm
Inner Diameter of Stator	60	mm
Number of Stator Slots	36	
Outer Diameter of rotor	120	mm
Inner Diameter of Rotor	106	mm
Length of Stator Core (Rotor)	40	mm
Stacking Factor	0.95	
Conductor per slot	52	
Stator slot fill	75.40%	
Operating Temperature	75	00C

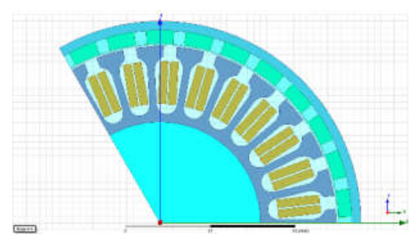

Alnico5

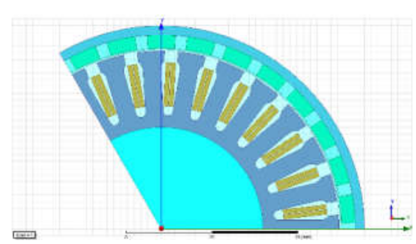

$ND_2FE_{14}B$

Figure 5a: 2D model of Radial flux outer rotor PMSG

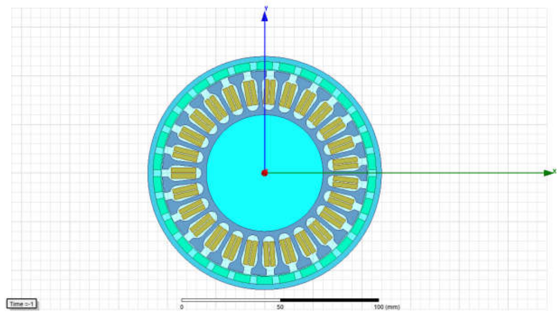

Alnico5

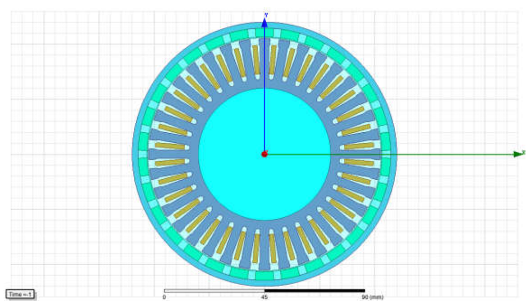

$ND_2FE_{14}B$

Figure 5b: 2D model of Radial flux outer rotor PMSG

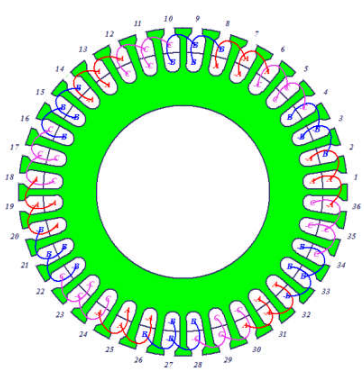

Figure 5c: Double layer 36 slot

The ANSYS Maxwell 2D has many solvers namely, electrostatic, magnetostatic, transient among others. Electrostatic solver is used to understand a static electric field, magnetostatic solvers are used to observe static magnetic fields in the machine. Transient solver allows the designer to observe and analyze the magnetic fields, energy, flux and many other parameters of the machine model at various time steps. The 2D is used in the analysis due to the symmetry of the structure of the model. It can be analyzed in 1/8 of the whole model to decrease the number of finite elements and save the simulation time (Niasar & Sabbaghean, 2015). The process of analyzing the electromagnetic field is by solving the classical Maxwell's equation (Aliabad & Ghoroghchian, 2015). The classical Maxwell's equations in differential form are written as follows:

$$\begin{cases} \nabla \times E = \dfrac{-\partial B}{\partial t} \\ \nabla \times H = J + \dfrac{\partial D}{\partial t} \\ \nabla \bullet D = \rho \\ \nabla \bullet B = 0 \end{cases} \tag{7}$$

where, E = Electric Field Intensity

D = Electric Flux Density

H = Magnetic Field Intensity

J = Electric Current Density

ρ = Electric Charge Density

B = Magnetic Field Density

The electric and magnetic field (E and H) and the corresponding flux density (D and B) quantities are not independent but are related by the equations as

$$\begin{cases} D = \varepsilon E \\ B = \mu H \end{cases} \tag{8}$$

where ε and μ are the permittivity and permeability respectively, of the material. In free space $\varepsilon = \varepsilon_0$ and $\mu = \mu_0$ which are related by

$$C_0^2 = \frac{1}{\mu_0 \varepsilon_0} \tag{9}$$

where, C_0 is the speed of light in free space (3×10^8 m/sec)

For a permanent magnet material, the expression becomes

$$\frac{B}{\mu_0} = \mu H + M_0 \tag{10}$$

where, M_0 is the remanent intrinsic magnetization and the electric field strength is further related by

$$J = \sigma E \qquad (11)$$

where σ is the conductivity of the material

Based on the equation (7) to (11) the magnetic field distribution of the generator was composed.

.

3 RESULTS AND DISCUSSION

The finite element model of the generator was developed and the geometry of the generator was drawn and the material properties assigned to the various regions of the model. The boundary conditions are applied and meshing was finally developed before the finite element solution was carried out using the solvers. Figure 7 shows the mesh distribution under the transient solver. The mesh is coarse at all parts of the geometry and no region with dense mesh. The three-phase stator current for Alnico5 and $Nd_2Fe_{14}B$ is shown in Figure 8 and Figure 9 with a magnitude of 0.36 A and 3.6 A respectively, which are practically sinusoidal. It can be observed from the figures that steady state response to three-phase current is achieved at around $20ms$. Figure 10 and Figure 11 shows the torque variation of the PM materials. The torque value in steady state is $-35Nm$ for Alnico5 and $-35.5Nm$ for $Nd_2Fe_{14}B$ with a pronounced cogging effect. An induced voltage of $1.7V$ was obtained for the Alnico PM material as shown in Figure 12, with a flux linkage shown in Figure 13. The voltage waveforms are clearly displaced by 120 degrees and there are non-distortions due to cogging torque issue. This validates the design worthiness. Figure 14 shows the flux density distribution, while Figure 15 gives the field intensity under the same transient solver used.

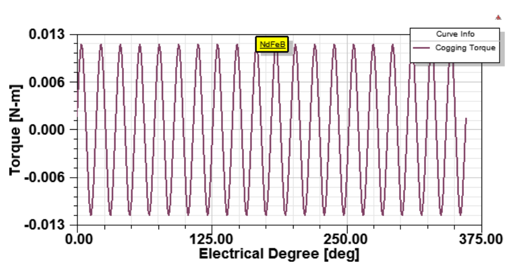

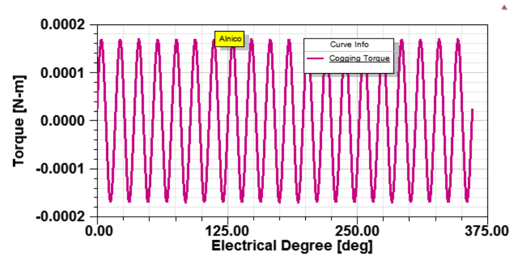

Figure 6: Cogging Torque in Two teeth

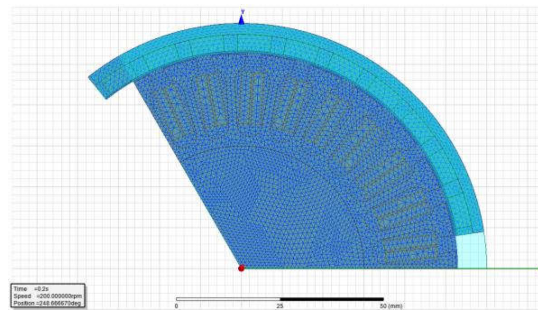

Figure 7: Geometry and FE mesh of half PMSG Alnico5 material

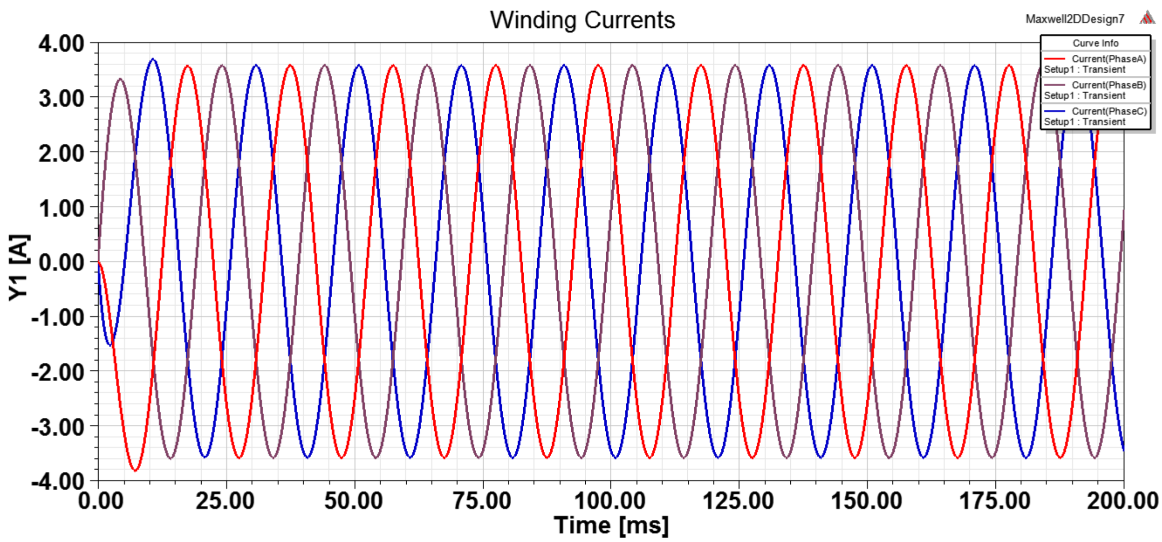

Figure 8: stator winding current of $Nd_2Fe_{14}B$

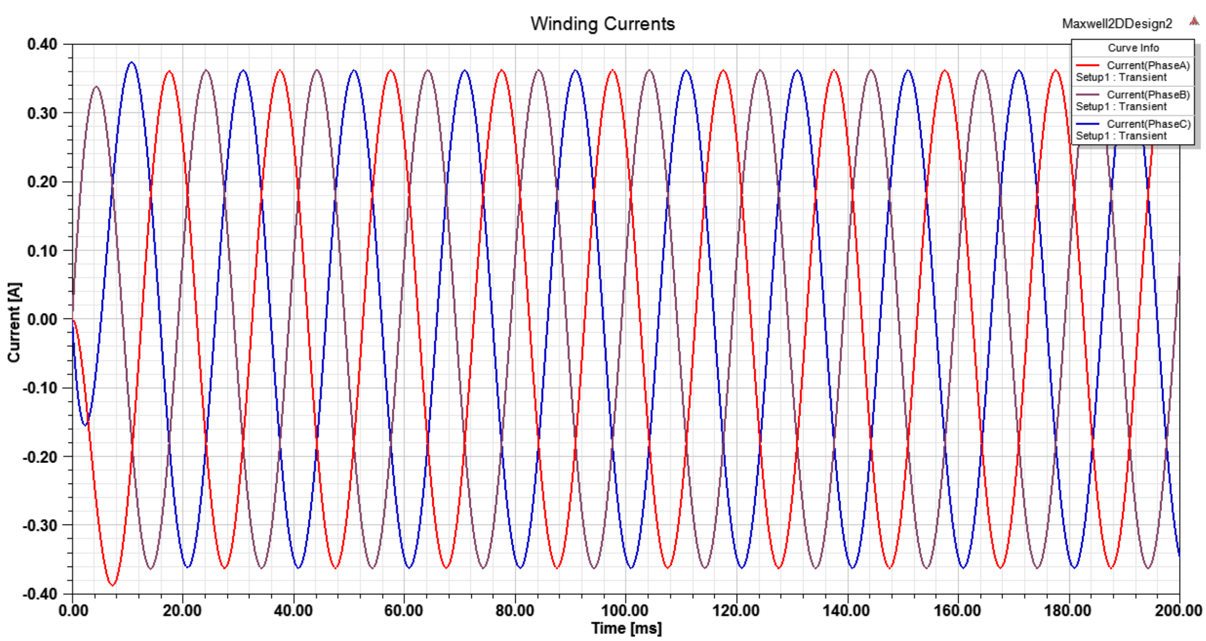

Figure 9: stator winding current of Alnico5

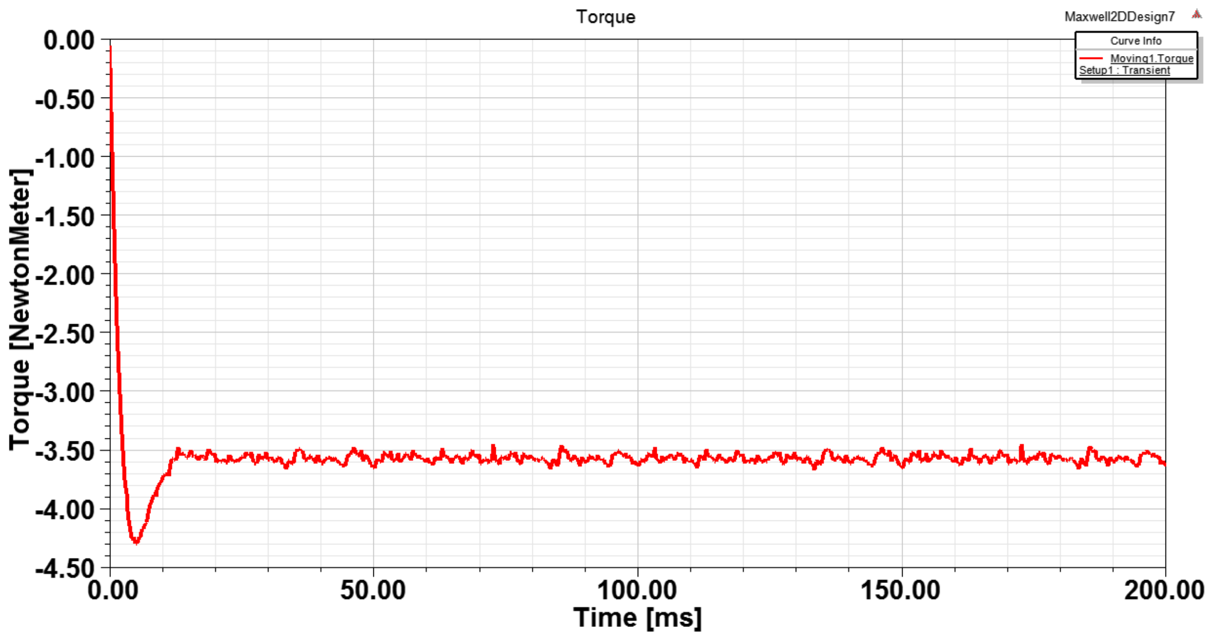

Figure 10: Electromagnetic torque variation of $Nd_2Fe_{14}B$

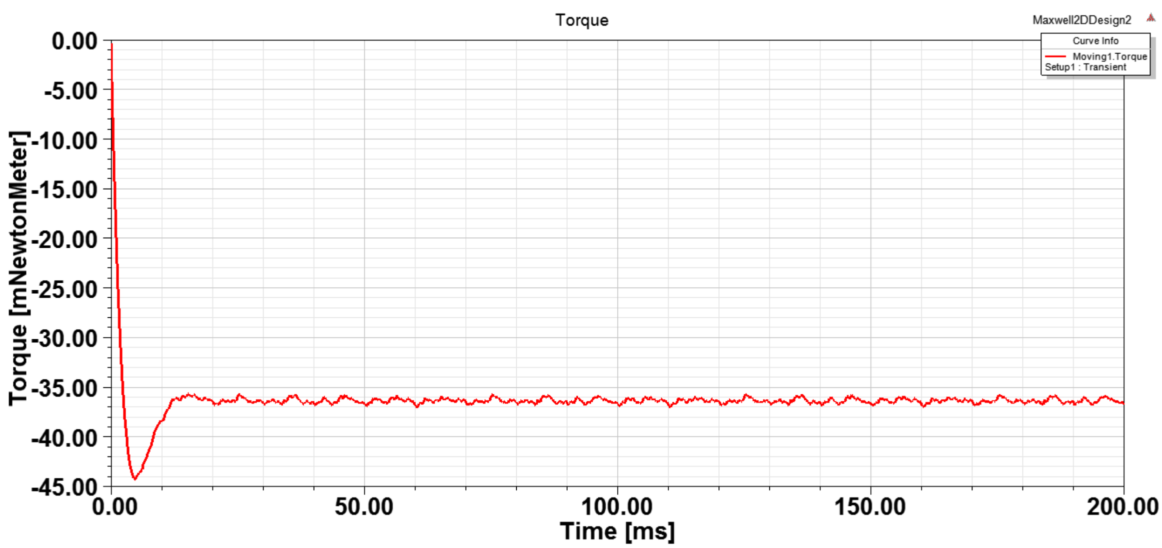

Figure 11: Electromagnetic torque variation of Alnico5

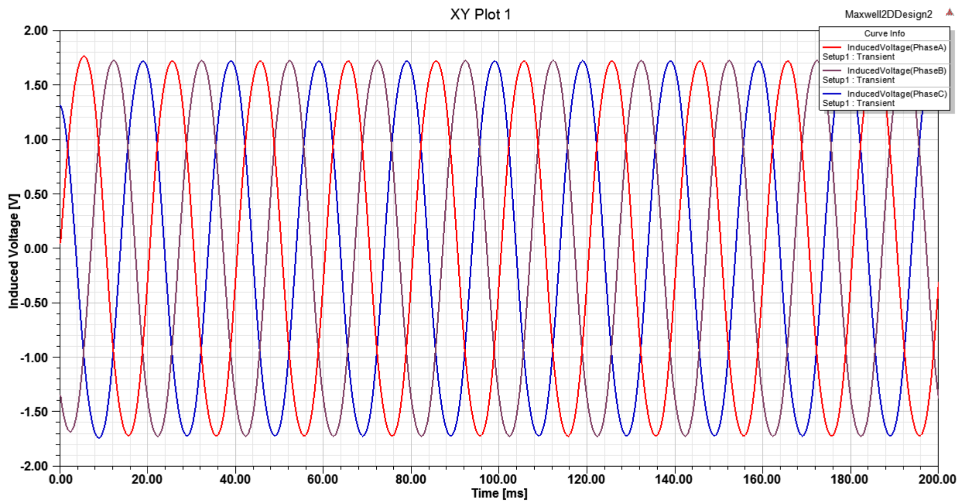

Figure 12: Induced Voltage of Alnico5.

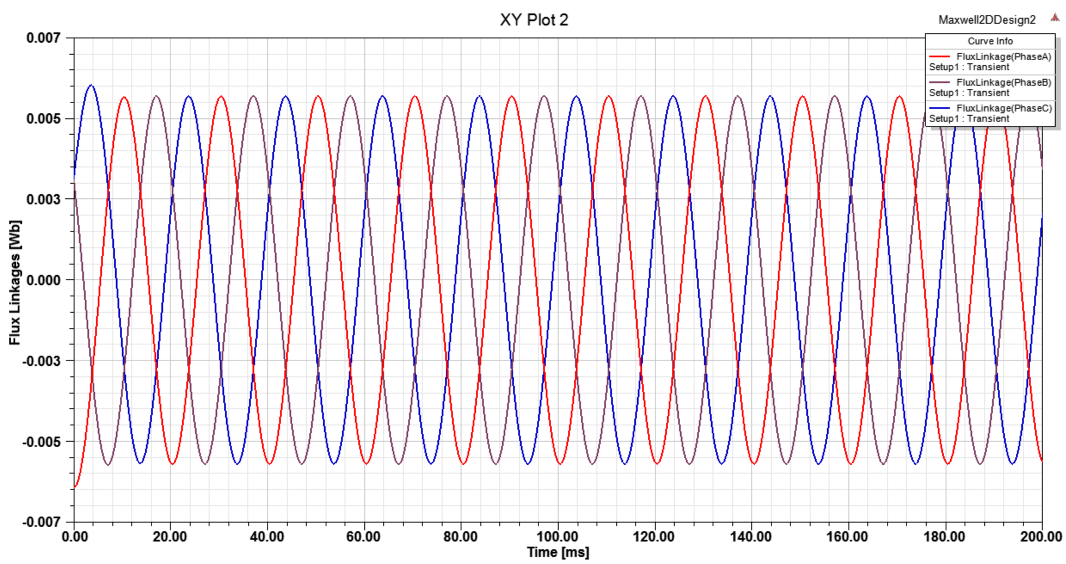

Figure 13: Flux Linkages of Alnico5

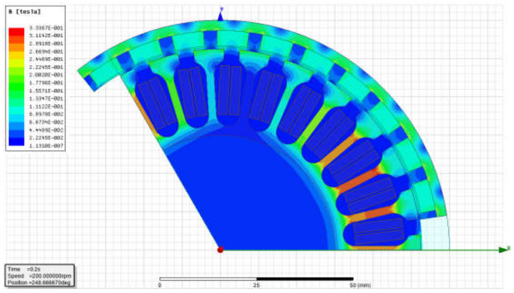

Figure 14: Flux density of Alnico5

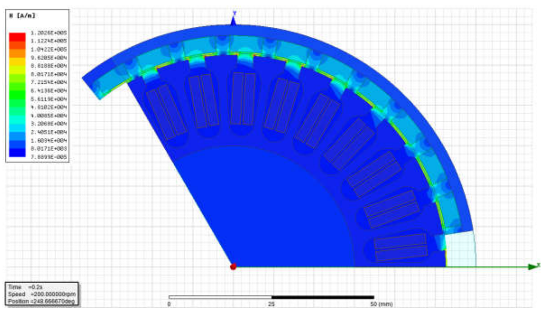

Figure 15: Magnetic field intensity of Alnico5

4 CONCLUSION

In this paper, a 2D model of a PMSG was developed and analyzed using the ANSYS Maxwell software. Two different PM materials, namely $Nd_2Fe_{14}B$ and Alnico were considered. Simulation results show that the Alnico model had better performance characteristics, due to its low cogging torque, low stator winding current and good torque performance characteristics. In addition, FEM has proved to be a viable tool for studying electromagnetic field analysis of PMSG for use in dedicated wind power generation systems. The results can assist designers in selecting better PM materials that can improve the generator design.

REFERENCE

Aliabad, A. D., & Ghoroghchian, F. (2015). Design and Analysis of a Two-Speed Line Start Synchronous Motor□: Scheme One. *IEEE Transaction on Energy Conversion*, *31*(1). http://doi.org/10.1109/TEC.2015.2481929

Cavagnino, A., Lazzari, M., Profumo, F., & Tenconi, A. (2002). A Comparison Between the Axial Flux and the Radial Flux Structures for PM Synchronous Motors. *IEEE Trans. on Inductry Application*, *38*(6), 1517–1524.

Chalmers, B. J., Wu, W., & Spooner, E. (1999). An Axial-flux Permanent-Magnet Generator for a Gearless Wind Energy System. *IEEE Transaction on Energy Conversion*, *14*(2), 251–257.

Chan, T. F., & Lai, L. L. (2007). An Axial-Flux Permanent-Magnet Synchronous Generator for a Direct-Coupled Wind-Turbine System. *IEEE Transaction on Energy Conversion*, *22*(1), 86–94.

Aliabad, A. D., & Ghoroghchian, F. (2015). Design and Analysis of a Two-Speed Line Start Synchronous Motor□: Scheme One. *IEEE Transaction on Energy Conversion*, *31*(1). http://doi.org/10.1109/TEC.2015.2481929

Cavagnino, A., Lazzari, M., Profumo, F., & Tenconi, A. (2002). A Comparison Between the Axial Flux and the Radial Flux Structures for PM Synchronous Motors. *IEEE Trans. on Inductry Application*, *38*(6), 1517–1524.

Chalmers, B. J., Wu, W., & Spooner, E. (1999). An Axial-flux Permanent-Magnet Generator for a Gearless Wind Energy System. *IEEE Transaction on Energy Conversion*, *14*(2), 251–257.

Chan, T. F., & Lai, L. L. (2007). An Axial-Flux Permanent-Magnet Synchronous Generator for a Direct-Coupled Wind-Turbine System. *IEEE Transaction on Energy Conversion*, *22*(1), 86–94.

Chen, J. Y., Nayar, C. V, & Xu, L. (1998). Design and Finite Element Analysis of an Outer-Rotor PM Generator for Directly- Coupled Wind Turbine Applications. In *IEEE conf Industry /Application* (pp. 387–394).

Chen, Y., Pillay, P., & Khan, A. (2004). PM Wind Generator Comparison of Different Topologies. In *IEEE Industry/Application conf. 2004 39th IAS Annual Meeting* (pp. 1405–1412). Seattle, WA, USA, USA: IEEE. http://doi.org/10.1109/IAS.2004.1348606

Gieras, J. F., & Wing, M. (2002). *Permanent Magnet Motor Technology: design and applications* (Vol. 113). http://doi.org/10.1201/9781420064414

Ionel, D. M., & Popescu, M. (2009). Finite Element Surrogate Model for Electric Machines with Revolving Field – Application to IPM Motors. In *IEEE Energy Conversion Congress and Exposition* (pp. 178–186).

Jeong, Y., Sul, S., Schulz, S. E., & Patel, N. R. (2005). Fault Detection and Fault-Tolerant Control of Interior Permanent-Magnet Motor Drive System for Electric Vehicle. *IEEE Trans. on Inductry Application*, *41*(1), 46–51.

Kyoung-Jin KoI, Seok-Myeong JangI, Ji-Hoon ParkI, Han-Wook ChoI, & Dae-Joon YouP. (2011). Electromagnetic Performance Analysis of Wind Power Generator With Outer Permanent Magnet

Rotor Based on Turbine Characteristics Variation Over Nominal Wind Speed. *IEEE Transaction on Magnetic*, *47*(10), 3292–3295.

Lampola, P., & Perho, J. (1996). Electromagnetic Analysis of A Low-Speed Permanent Magnet Wind Generator. In *IEEE, Opportunities and Advances in International Power Generation Conf. publ. No. 419* (pp. 55–58). Durham, UK. http://doi.org/10.1049/cp:19960118

Li, H., & Chen, Z. (2008). Overview of different wind generator systems and their comparisons. *IET Renewable Power Generation*, *2*(2), 123–138. http://doi.org/10.1049/iet-rpg:20070044

Niasar, A. H., & Sabbaghean, A. (2015). Design and implementation of a low-cost maximization power conversion system for brushless DC generator. *AIN SHAMS ENGINEERING JOURNAL*. http://doi.org/10.1016/j.asej.2015.11.001

Ong, C. . (1998). *Dynamic Simulation of Electric machinery using Matlab/Simulink*. New Jersey: PrenticeHall PTR.

Parviainen, A., Pyrhönen, J., & Kontkanen, P. (2005). Axial Flux Permanent Magnet Generator with Concentrated Winding for Small Wind Power Applications. In *IEEE Electric Machine and Drives Conf* (pp. 1187–1191). San Antonio, TX, USA: IEEE. http://doi.org/10.1109/IEMDC.2005.195871

Pena, R. S., Cardenas, R. J., Asher, G. M., & Clare, J. C. (2000). Vector controlled induction machines for stand-alone wind energy applications. In *Industry Applications Conference, 2000. Conference Record of the 2000 IEEE* (pp. 1409–1415). Rome, Italy. http://doi.org/10.1109/IAS.2000.882069

Sarhan M. Musa. (2012). *Computational Finite Element Methods in Nanotechnology*. CRC Press Taylor & Francis Group.